

# Design, synthesis, and photoelectric properties of V-shaped organic fluorescent compounds with a 1,3,4-oxadiazole moiety

Journal of Chemical Research  
2019, Vol. 43(1-2) 3-7  
© The Author(s) 2019  
Article reuse guidelines:  
sagepub.com/journals-permissions  
DOI: 10.1177/1747519819831881  
journals.sagepub.com/home/chl



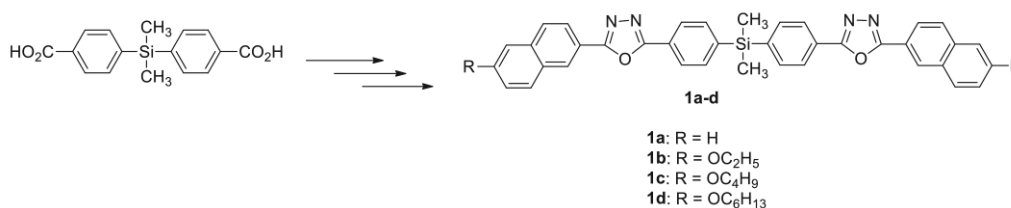
Rui-Bin Hou<sup>1,2</sup>, Ji-Ying Su<sup>1,2</sup>, Ling-Ling Zhang<sup>1</sup>,  
Dong-Feng Li<sup>1</sup> and Yan Xia<sup>1,2</sup>

## Abstract

A series of symmetric, silicon-linked organic fluorescent compounds with two electron-deficient 1,3,4-oxadiazole units were synthesized and characterized. The compounds possessed a V-shaped structure with a silicon atom, which weakened  $\pi$ - $\pi$  stacking, promoting aggregation-induced emission. The compounds were fluorescent in both solution and solid-state thin films. The efficient fluorescent behavior of the materials was confirmed through optical and electrochemical measurements. The compounds displayed excellent thermal stability, with decomposition temperatures exceeding 400 °C. Amorphous films of the compounds possessed high morphological stability. These results indicate that the compounds may be promising emissive and electron-transporting materials.

## Keywords

1,3,4-oxadiazoles, electron-transporting materials, fluorescent materials, thermal stability, V-shaped structure



## Introduction

Organic fluorescent materials have been the subject of great interest because of their potential applications in many aspects of modern life, such as lighting, displays, bioprobes, and chemosensors.<sup>1-5</sup> Generally, the luminescence properties of organic molecules in the solid state are determined mainly by their chemical structures. Most fluorescent organic molecules with highly conjugated planar structures emit reasonably intense fluorescence in dilute solutions but emit weak or nonexistent emission in the solid state because of aggregation-induced quenching.<sup>6-9</sup> However, some groups have recently reported the unique phenomenon of aggregation-induced emission (AIE).<sup>10,11</sup> Propeller-shaped molecules such as tetraphenylethene, hexaphenylsilole, and quinoline-malononitrile, along with their derivatives, are known to display AIE.<sup>12-17</sup> Molecular design optimization can be used to increase molecular luminous efficiency and stability, leading to organic light-emitting diodes (OLEDs) with improved optoelectronic properties.<sup>18-21</sup>

Considering all organic luminescent materials, silicon (Si)-based compounds have been reported to perform well

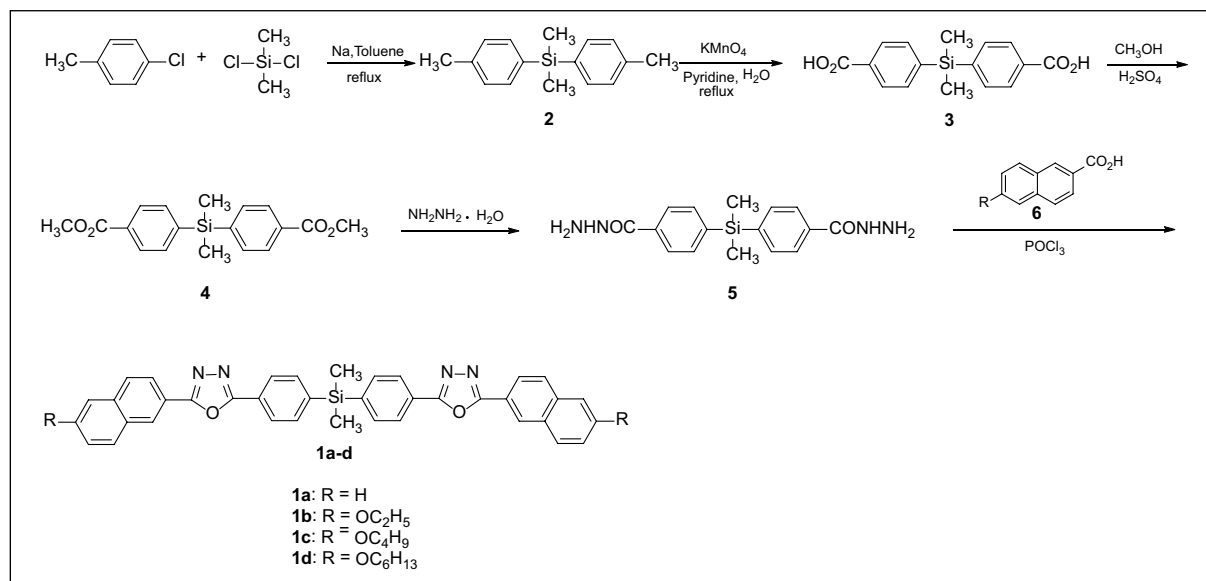
in optical applications because of their high brightness, thermal stability, and amorphous film-forming capability.<sup>22-24</sup> Si-based tetrahedral organic molecules and polymers have been intensively investigated as electroluminescent materials. For example, Partee et al.<sup>25</sup> and Zhen et al.<sup>26</sup> recently reported a series of tetrahedral luminescent materials with SiAr<sub>4</sub> cores. Meanwhile, 1,3,4-oxadiazoles are classic heterocyclic compounds that have also attracted substantial interest for use in OLEDs because of their favorable electronic transmission properties. Many kinds of oxadiazole-based materials have been synthesized and used in different applications, and some are considered to be potential blue emitters for OLEDs.<sup>27,28</sup>

<sup>1</sup>Key Laboratory School of Chemistry and Life Science, Changchun University of Technology, Changchun, P.R. China

<sup>2</sup>Advanced Institute of Materials Science, Changchun University of Technology, Changchun, P.R. China

## Corresponding authors:

Dong-Feng Li and Yan Xia, Key Laboratory School of Chemistry and Life Science, Changchun University of Technology, Changchun, 130012, P.R. China. Emails: lidongfeng@ccut.edu.cn; hzm20130521@163.com



Scheme 1. Synthetic route of **1a-d**.

## Results and discussion

Continuing our interest in V-shaped luminescent materials,<sup>29,30</sup> in this article, we report the development of a series of V-shaped fluorescent molecules (**1a-d**) containing a naphthalene-linked 1,3,4-oxadiazole and an Si core atom, which weakens  $\pi$ - $\pi$  stacking interactions. The length of the alkoxy chain attached to naphthalene was changed to study the effect on the photochemical and electrochemical properties of the materials in solution and in the solid state.

Starting compounds **2-5** were synthesized according to the reported methods.<sup>31,32</sup> The synthetic procedure followed to obtain target compound **1a-d** is summarized in Scheme 1, and the details are given in the section "Experimental." An important intermediate (**5**) with a silylbenzohydrazide moiety was prepared quantitatively by the reaction of **4** with excess hydrazine monohydrate under reflux. The reaction of **5** and 2-naphthoic acid **6a** or 6-alkoxy-2-naphthoic acid **6b-d** in phosphorus oxychloride under reflux gives compound **1a-d** as white crystals in yields of 32%–39%. The structures of **1a-d** were characterized by <sup>1</sup>H and <sup>13</sup>C nuclear magnetic resonance (NMR) spectroscopy, mass spectrometry, and elemental analysis.

The ultraviolet (UV)-Vis absorption properties of compounds **1a-d** in CHCl<sub>3</sub> solution are presented in Figure 1. The absorption spectra contain a wide peak in the region of 315–330 nm originating from the  $\pi$ - $\pi^*$  absorption of the conjugated naphthalene-phenyl 1,3,4-oxadiazole moiety. The absorption spectra of compounds **1b-d** possessing alkoxy groups displayed bathochromic shifts of 15 nm compared with that of compound **1a** without a substituent. These results illustrate that the alkoxy chain can lower the energy of the  $\pi$ - $\pi^*$  transition of the molecules. The optical band gaps ( $E_g^{\text{opt}}$ ) of the series were calculated from the relevant absorption onsets and found to be 3.88, 3.76, 3.76, and 3.76 eV, respectively.<sup>33</sup>

The photoluminescence (PL) spectra of compounds **1a-d** in CHCl<sub>3</sub> solution and in solid-state films obtained by spin-coating a CHCl<sub>3</sub> solution are shown in Figure 2.

The PL spectrum of compound **1a** in CHCl<sub>3</sub> contains two emission peaks at around 340 and 400 nm (Figure 2(a)). The emission spectra of compounds **1b-d** in CHCl<sub>3</sub> also contain one similar broad peak. Interestingly, the emission maxima of compounds **1b-d** are red-shifted to 382 nm compared with that of **1a** because of the alkoxy chain substituents. The fluorescence quantum yields (QYs) of **1a-d** measured at room temperature in dilute CHCl<sub>3</sub> were moderate with the values of 0.71, 0.72, 0.72, and 0.72, respectively, compared with the PL intensity of a standard solution of quinine sulfate (QY=0.55). The emission spectra of the films were quite different to those for the solutions with regard to the two main emission peaks, as demonstrated in Figure 2(b). The emission maxima of compounds **1b-d** red-shifted with increasing length of the alkyl chain. The intensity of one of the emission peaks increased, while that of the other decreased as the alkyl chain lengthened. This phenomenon may originate from the dihedral angle of the molecules increasing with the length of the alkoxy chain.

The electrochemical properties of **1a-d** in dimethylformamide (DMF) were investigated by cyclic voltammetry (CV) as summarized in Figure 3 and Table 1. Figure 3 displays representative CV traces for the oxidation and reduction of **1c**. The CV curves reveal that **1c** undergoes a quasi-reversible reduction at the cathodic potential associated with the reduction of an electron-deficient oxadiazole moiety to form an anion radical. Compound **1c** also exhibits an irreversible oxidation process corresponding to the removal of an electron from the peripheral phenyl group to give a radical cation.

Calculations of **1a-d** were carried out using the Gaussian 09 (G09) package.<sup>35</sup> GaussView 5.0.8 was used for the visualization of the structures and orbital manipulation. The calculated highest occupied molecular orbital (HOMO), lowest unoccupied molecular orbital (LUMO), and energy gap for each of **1a-d** are displayed in Figure 4. The calculated energy gaps agreed well with the experimental photophysical data, suggesting that density functional theory (DFT) calculations

can be used to predict the photophysical behavior of these complexes to some extent. The electron density of the HOMO of **1a–d** is predominantly localized on the naphthalene donor moiety and diffusively distributed over the  $\pi$ -conjugation onto the 1,3,4-oxadiazole ring.

The thermal stability of a material is important for device longevity. Figure 5 and Table 1 show the results of thermogravimetric analysis (TGA) of compounds **1a–d**. The TGA analysis revealed that the compounds possessed relatively high thermal stability with an initial weight loss (5%) temperature of 400–434 °C. The glass transition temperature ( $T_g$ ) values of **1a–d** were in the range of 87–100 °C. The thermal stabilities of the compounds progressively decreased as the substituent alkoxy chain lengthened. The high thermal stability of **1a–d** would benefit the formation of amorphous films.

In summary, we developed a facile and effective method to synthesize V-shaped organic fluorescent compounds. These synthesized compounds do not aggregate in the condensed state as shown by their similar properties either in solution or in film states. These emitters are solution processable and exhibit good film-forming ability as well as high thermal stability, making them attractive for use in OLEDs.

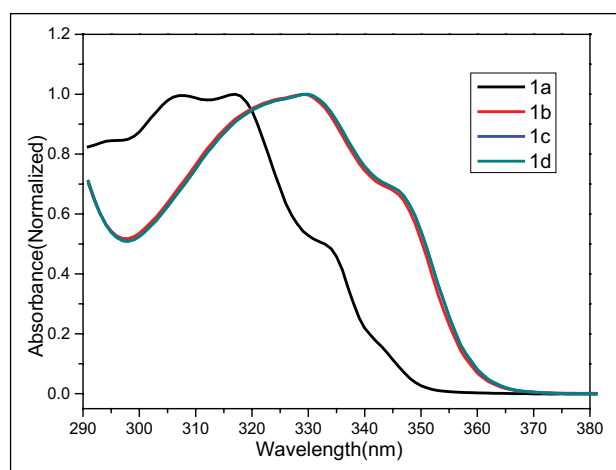


**Figure 1.** UV-Vis absorption spectra of compounds **1a–d** in  $\text{CHCl}_3$  solution. UV: ultraviolet.

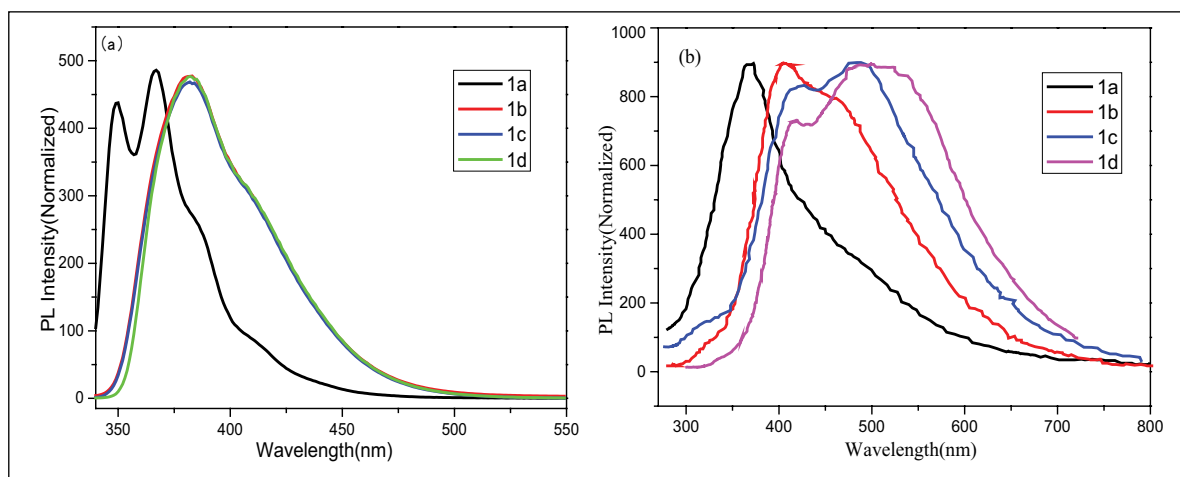


**Figure 2.** Normalized PL spectra of compounds **1a–d** in (a)  $\text{CHCl}_3$  and (b) as films. PL: photoluminescence.

## Experimental

NMR spectra were recorded in  $\text{CDCl}_3$  with a Bruker AV-400 spectrometer. Chemical shifts were referenced relative to tetramethylsilane ( $\delta_{\text{H}}/\delta_{\text{C}}=0$ ). Infrared (IR) spectra were recorded on a Perkin Elmer 2400 spectrophotometer (using KBr pressed disks). Mass spectra were collected on an Autoflex Speed™ matrix-assisted laser desorption/ionization time-of-flight (MALDI-TOF) spectrometer. Elemental analyses were performed on an Elementar Vario EL CHN elemental analyzer. UV-Vis spectra were recorded on a Lambda 25 spectrophotometer in  $\text{CHCl}_3$ . Fluorescence spectra were obtained from a Shimadzu RF-5301PC fluorescence spectrophotometer in  $\text{CHCl}_3$ . CV was conducted using a CHI 852C instrument with  $10^{-3}$  M solutions using  $\text{CH}_2\text{Cl}_2$  as the solvent ( $10^{-3}$ ) and containing 0.1 M  $\text{Bu}_4\text{NPF}_6$  as the supporting electrolyte. Counter and working electrodes consisted of a Pt wire and a Pt disk, respectively, and the reference electrode was Ag/AgCl. The thermal stability of the target compounds was characterized using a Diamond TG/DTA thermogravimetric analyzer. Starting compounds **2–5** were synthesized according to the methods described in the literature.<sup>31,32</sup> The commercially available 6-alkoxy-2-naphthoic acids **6b–d** were purchased from J&K Chemical Company.

### General procedure for the preparation of compounds **1a–d**

A mixture of the appropriate 2-naphthoic acid **6a–d** (2 mmol), 4,4'-(dimethylsilaneyl)di(benzohydrazide) (1 mmol), and phosphorus oxychloride (10 mL) was heated under reflux for 16 h under  $\text{N}_2$ , then cooled to room temperature, and poured onto crushed ice. The resulting dark green solid precipitate was filtered and then washed thoroughly with distilled ice water. The solid was recrystallized from DMF/ $\text{H}_2\text{O}$  to obtain the pure final compound.

*Dimethylbis{4-[5-(naphthalen-2-yl)-1,3,4-oxadiazol-2-yl]phenyl}silane (1a)*: White solid (Yield: 32%), m.p. 249.60 °C (by differential scanning calorimetry (DSC));  $^1\text{H}$  NMR (400 MHz,  $\text{CDCl}_3$ ):  $\delta$  0.69 (s, 6H), 7.55–7.64 (m, 4H), 7.74 (d,  $J=8.0$  Hz, 4H), 7.88–7.94 (m, 2H), 8.00 (d,

$J=8.0$  Hz, 4H), 8.15–8.25 (m, 6H), 8.64 (s, 2H);  $^{13}\text{C}$  NMR (100 MHz,  $\text{CDCl}_3$ ):  $\delta$  -2.50, 121.38, 123.45, 124.92, 126.39, 127.31, 127.56, 128.18, 129.03, 129.26, 133.09, 134.95, 134.98, 142.52, 164.85, 165.09; IR (KBr),  $\nu_{\text{max}}/\text{cm}^{-1}$ : 2968, 1626, 1497, 1408, 1346, 1292, 1250, 1118,

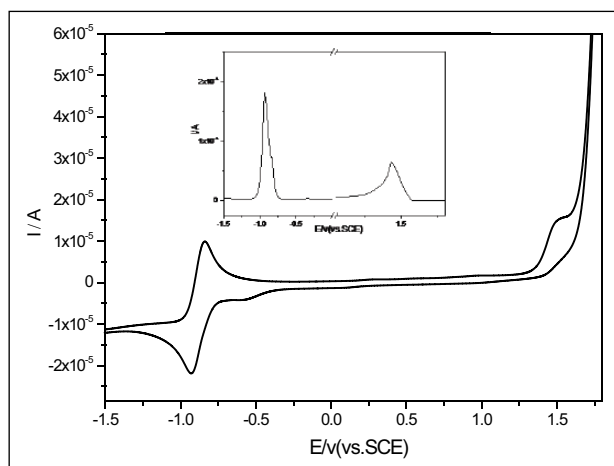


**Figure 3.** CV of **1c** ( $1 \times 10^{-3}$  M) in 0.1 M tetrabutylammonium hexafluorophosphate in  $\text{CH}_2\text{Cl}_2$  at a scan rate of  $0.1 \text{ V s}^{-1}$  (inset: differential pulse voltammogram of **1c** under the same conditions). CV: cyclic voltammetry.

1079, 830, 779; MALDI-TOF MS  $m/z$  (%) = 601.1372 ( $M+1$ , 100); anal. calcd for  $\text{C}_{38}\text{H}_{28}\text{N}_4\text{O}_2\text{Si}$ : C, 75.97; H, 4.70; found: C, 75.62; H, 4.76%.

**Bis{4-[5-(6-ethoxynaphthalen-2-yl)-1,3,4-oxadiazol-2-yl]phenyl}dimethylsilane (1b):** White solid (Yield: 35%), m.p.  $227.21^\circ\text{C}$  (by DSC);  $^1\text{H}$  NMR (400 MHz,  $\text{CDCl}_3$ ):  $\delta$  0.67 (s, 6H), 1.50 (t,  $J=6.8$  Hz, 6H), 4.18 (q,  $J=6.8$  Hz, 4H), 7.16 (d,  $J=2.0$  Hz, 2H), 7.21 (dd,  $J=8.9$ , 2.3 Hz, 2H), 7.71 (d,  $J=8.0$  Hz, 4H), 7.85 (t,  $J=9.8$  Hz, 4H), 8.11–8.19 (m, 6H), 8.53 (s, 2H);  $^{13}\text{C}$  NMR (100 MHz,  $\text{CDCl}_3$ ):  $\delta$  -2.50, 14.89, 63.86, 106.90, 119.01, 120.49, 123.99, 124.99, 126.31, 127.34, 127.88, 128.40, 130.52, 134.95, 136.55, 142.37, 158.90, 164.57, 165.27; IR (KBr),  $\nu_{\text{max}}/\text{cm}^{-1}$ : 2981, 1629, 1555, 1543, 1504, 1399, 1259, 1209, 1115, 1045, 811, 779, 731; MALDI-TOF MS  $m/z$  (%) = 689.1630 ( $M+1$ , 100); anal. calcd for  $\text{C}_{42}\text{H}_{36}\text{N}_4\text{O}_4\text{Si}$ : C, 73.23; H, 5.27; found: C, 73.19; H, 5.32%.

**Bis{4-[5-(6-butoxynaphthalen-2-yl)-1,3,4-oxadiazol-2-yl]phenyl}dimethylsilane (1c):** White solid (Yield: 39%), m.p.  $214.16^\circ\text{C}$  (by DSC);  $^1\text{H}$  NMR (400 MHz,  $\text{CDCl}_3$ ):  $\delta$  0.68 (t, 6H), 1.02 (t,  $J=7.2$  Hz, 6H), 1.49–1.62 (m, 4H), 1.81–1.92 (m, 4H), 4.12 (t,  $J=6.8$  Hz, 4H), 7.18 (d,  $J=1.6$  Hz, 2H), 7.23 (dd,  $J=8.8$  Hz, 2.4 Hz, 2H), 7.72 (d,  $J=8.0$  Hz, 4H), 7.86 (t,  $J=9.8$  Hz, 4H), 8.13–8.21 (m, 6H), 8.55 (s, 2H);  $^{13}\text{C}$  NMR (100 MHz,  $\text{CDCl}_3$ ):  $\delta$  -2.49,

**Table I.** Photophysical, physical, and electrochemical data.

Compound	$^a\lambda_{\text{max,Abs}}$ (nm)	$^a\lambda_{\text{max,em}}$ (nm)	$\Phi_{\text{F}}$	$E_{\text{red/peak}}$ (V)	$E_{\text{I}^{\text{ox/peak}}}$ (V)	$E_{\text{g}}^{\text{opt}}$	$E_{\text{g}}^{\text{Cal}}$	$T_{\text{d}}$	$T_{\text{g}}$
1a	316	366	0.712	-0.65	1.36	3.98	4.43	416	87.2
1b	329	382	0.715	-0.88	1.53	3.83	4.15	409	99.1
1c	330	382	0.716	-0.89	1.53	3.82	4.15	406	95.8
1d	330	382	0.716	-0.89	1.51	3.82	4.16	402	92.6

$\Phi_{\text{F}}$  is the fluorescence quantum yield, which was measured in  $\text{CHCl}_3$  using quinine sulfate as a standard ( $\Phi_{\text{F}}=0.55$ );<sup>34</sup>  $E_{\text{g}}^{\text{opt}}$  is the optical band gap, which was calculated using  $E_{\text{g}}=1240/\lambda_{\text{abs onset}}$ ;  $E_{\text{g}}^{\text{Cal}}$  is the calculated energy gap;  $T_{\text{d}}$  represents the temperature at which 5% weight loss occurred;  $T_{\text{g}}$  represents the glass transition temperature.

<sup>a</sup>Measured in  $\text{CHCl}_3$ .

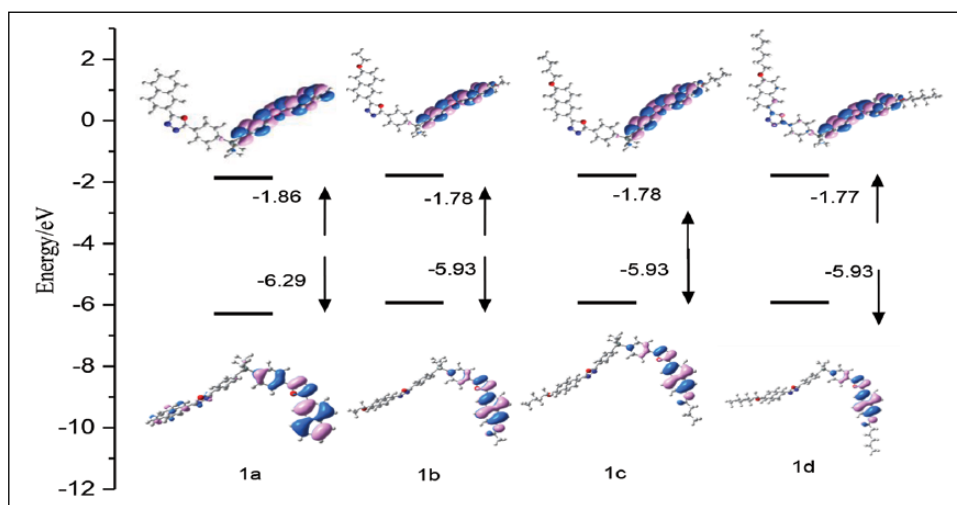


**Figure 4.** Contour plots of the HOMO and LUMO for complexes **1a–d**.

HOMO: highest occupied molecular orbital; LUMO: lowest unoccupied molecular orbital.

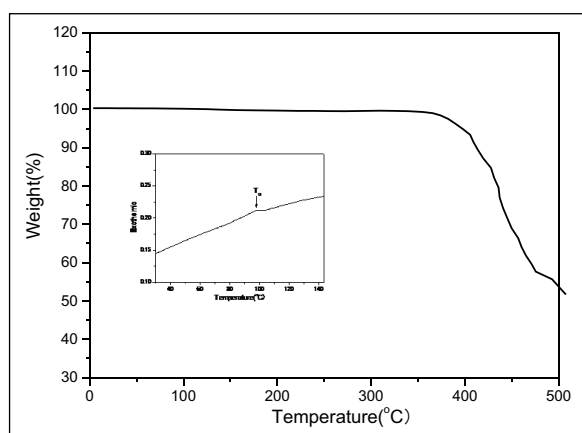


**Figure 5.** Thermal gravimetric analysis and differential scanning calorimetry thermograms of **1b**.

13.99, 19.46, 31.40, 68.11, 106.92, 119.00, 120.52, 124.00, 125.02, 126.32, 127.34, 127.87, 128.39, 130.49, 134.95, 136.58, 142.36, 159.13, 164.57, 165.29; IR (KBr),  $\nu_{\max}/\text{cm}^{-1}$ : 2962, 1635, 1559, 1500, 1394, 1275, 1210, 1005, 810, 736; MALDI-TOF MS  $m/z$  (%) = 745.2318 ( $M+ + 1$ , 100); anal. calcd for  $\text{C}_{46}\text{H}_{44}\text{N}_4\text{O}_4\text{Si}$ : C, 74.17; H, 5.95; found: C, 74.13; H, 5.98%.

*Bis*{4-[5-(6-hexyloxynaphthalen-2-yl)-1,3,4-oxadiazol-2-yl]phenyl}dimethylsilane (**1d**): White solid (Yield: 39%), m.p. 199.65°C (by DSC);  $^1\text{H}$  NMR (400 MHz,  $\text{CDCl}_3$ ):  $\delta$  0.68 (s, 6H), 0.92 (t,  $J=7.2$  Hz, 6H), 1.32–1.42 (m, 8H), 1.45–1.53 (m, 4H), 1.79–1.91 (m, 4H), 4.10 (t,  $J=6.8$  Hz, 4H), 7.16 (d,  $J=2.4$  Hz, 2H), 7.22 (dd,  $J=9.0, 2.4$  Hz, 2H), 7.71 (d,  $J=8.0$  Hz, 4H), 7.85 (t,  $J=9.6$  Hz, 4H), 8.15–8.19 (m, 6H); 8.53 (s, 2H);  $^{13}\text{C}$  NMR (100 MHz,  $\text{CDCl}_3$ ):  $\delta$  -2.49, 14.17, 22.76, 25.93, 29.31, 31.75, 68.43, 106.93, 119.00, 120.53, 124.00, 125.02, 126.32, 127.34, 127.87, 128.39, 130.49, 134.95, 136.58, 142.36, 159.12, 164.57, 165.29; IR (KBr),  $\nu_{\max}/\text{cm}^{-1}$ : 2967, 1629, 1554, 1499, 1389, 1265, 1210, 1067, 1025, 815, 736; MALDI-TOF MS  $m/z$  (%) = 801.3242 ( $M+ + 1$ , 100); anal. calcd for  $\text{C}_{50}\text{H}_{52}\text{N}_4\text{O}_4\text{Si}$ : C, 74.97; H, 6.54; found: C, 74.92; H, 5.71%.

The  $^1\text{H}$  and  $^{13}\text{C}$  NMR spectra, TOF-MS data, cyclic voltammograms, and TGA data for **1a–d** in detail can be found in Supplemental material.

### Acknowledgements

We thank Natasha Lundin, PhD, from Liwen Bianji, Edanz Editing China (www.liwenbianji.cn/ac), for editing the English text of a draft of this manuscript.

### Declaration of conflicting interests

The author(s) declared no potential conflicts of interest with respect to the research, authorship, and/or publication of this article.

### Funding

The author(s) disclosed receipt of the following financial support for the research, authorship and/or publication of this article: This work was supported by the National Science Foundation of China

(No. 21442004 and 21502008) and the Education Office of Jilin province (No. 2016320).

### Supplemental material

The supplemental material with  $^1\text{H}$  and  $^{13}\text{C}$  NMR spectra, TOF-MS data, cyclic voltammograms, and TGA data for **1a–d** is available online.

### References

1. Tang CW and VanSlyke SA. *Appl Phys Lett* 1987; 51: 913.
2. Yang Y, Zhao Q, Feng W, et al. *Chem Rev* 2013; 113: 192.
3. Guo Z, Park S, Yoon J, et al. *Chem Soc Rev* 2014; 43: 16.
4. Xu C, Li H, Kan Y, et al. *Biosens Bioelectron* 2015; 72: 275.
5. Feng X, Tian P, Xu Z, et al. *J Org Chem* 2013; 78: 11318.
6. Birks JB. *Photophysics of aromatic molecules*. London: Wiley, 1970.
7. Mancin F, Scrimin P, Tecilla P, et al. *Coordin Chem Rev* 2009; 253: 2150.
8. Thomas SW, Joly GD and Swager TM. *Chem Rev* 2007; 107: 1339.
9. Chen CT. *Chem Mater* 2004; 16: 4389.
10. Hong Y, Lam JWY and Tang BZ. *Chem Soc Rev* 2011; 40: 5361.
11. Yuan WZ, Zhao H, Shen XY, et al. *Macromolecules* 2009; 42: 9400.
12. Zhang T, Jiang Y, Niu Y, et al. *J Phys Chem A* 2014; 118: 9094.
13. Zhang X, Ma Z, Yang Y, et al. *J Mater Chem C* 2014; 2: 8932.
14. Li H, Zhang X, Chi Z, et al. *Org Lett* 2011; 13: 556.
15. Zhang R, Gao M, Bai S, et al. *J Mater Chem B* 2015; 3: 1590.
16. Fu Y, Qiu F, Zhang F, et al. *Chem Commun* 2015; 51: 5298.
17. Liu G, Chen D, Kong L, et al. *Chem Commun* 2015; 51: 8555.
18. He CY, Guo HQ, Peng QM, et al. *J Mater Chem C* 2015; 3: 9942.
19. Yang XL, Xu XB and Zhou GJ. *J Mater Chem C* 2015; 3: 913.
20. Li YC, Wang ZH, Li XL, et al. *Chem Mater* 2015; 27: 1100.
21. Li J, Ding DX, Tao YT, et al. *Adv Mater* 2016; 28: 3122.
22. Lyu YY, Kwak J, Kwon O, et al. *Adv Mater* 2008; 20: 2720.
23. May F, Al-Helwi M, Baumeier B, et al. *J Am Chem Soc* 2012; 134: 13818.
24. Zhao Z, He B and Tang BZ. *Chem Sci* 2015; 6: 5347.
25. Partee J, Frankevich EL, Uhlhorn B, et al. *Phys Rev Lett* 1999; 82: 3673.
26. Zhen CG, Chen ZK, Liu QD, et al. *Adv Mater* 2009; 21: 2425.
27. Kaminorz Y, Schulz B, Schrader S, et al. *Synthetic Met* 2001; 122: 115.
28. Olivier Y, Moral M, Muccioli L, et al. *J Mater Chem C* 2017; 5: 5718.
29. Li D, Huang Z, Shang X, et al. *Tetrahedron* 2015; 71: 2680.
30. Zhang L, Xia Y, Li D, et al. *Tetrahedron* 2016; 72: 7438.
31. Tang HY, Song NH, Gao ZH, et al. *Polymer* 2007; 48: 129.
32. Ren XJ, Wang L, Gao L, et al. *Chinese J Org Chem* 2009; 29: 1147.
33. Kochapradist P, Sunonnamb T, Prachumrak N, et al. *Tetrahedron Lett* 2014; 55: 6689.
34. Kartens T and Kobs K. *J Phys Chem* 1980; 84: 1871.
35. Frisch MJ, Trucks GW, Schlegel HB, et al. *GAUSSIAN 09 (Revision B.01)*. Wallingford, CT: Gaussian, Inc., 2010.